Journal of
Marine Science and Engineering

MDPI

Article

Characteristics of Early Neoproterozoic Stromatolites from Southern Liaoning, North China: Insights into the Formation of Stromatolites

Yongli Zhang [1], Guanming Lai [1,*], Enpu Gong [1,*], Dingcheng Yuan [1], Mark A. Wilson [2] and Yu Li [1]

[1] College of Resources and Civil Engineering, Northeastern University, Shenyang 110819, China; zhangyongli@mail.neu.edu.cn (Y.Z.); 2100980@stu.neu.edu.cn (D.Y.); liyu_jasmine@163.com (Y.L.)
[2] Department of Earth Sciences, The College of Wooster, Wooster, OH 44691, USA; mwilson@wooster.edu
* Correspondence: guanmingl@163.com (G.L.); gongep@mail.neu.edu.cn (E.G.)

Abstract: Stromatolites, among the earliest fossils in Earth's history, are widely distributed on the margins of the North China Precambrian carbonate platform. The formation processes of stromatolites reveal the biomineralization and evolution of early life in the Precambrian. The well-preserved stromatolitic dolostones recorded in the Ganjingzi Formation are developed around Yuanjiagou village, in southern Liaoning Province. The morphology of the Ganjingzi stromatolites manifests in stratiform, columnar, and domal forms. A tripartite lamina structure including light laminae and two types of dark laminae is observed in thin sections. The origins of dark laminae were related to microbial metabolism, while the light laminae were the result of the recrystallization of synsedimentary marine cement. Hardground substrate and carbonate fragments were suitable for microbes to colonize, suggesting that microbes can adapt to various current energy settings. A comparison of the growth environment, morphology, and laminae features between the Ganjingzi stromatolites and modern carbonate stromatolites from Hamelin Pool and Lagoa Vermelha suggest that the Ganjingzi stromatolites may have been formed in a restricted tidal-flat setting with high salinity and evaporation. The role of microbes that form modern stromatolites in inducing precipitation of carbonate or binding sediments, might contribute to the formation of the Ganjingzi stromatolites. The formation process of the Ganjingzi stromatolites indicates that the microbial communities, favorable substrate, and synsedimentary marine cement were the key factors in promoting the development of the Neoproterozoic stromatolites on the northeastern margin of the North China Craton.

Keywords: stromatolites; Ganjingzi formation; Neoproterozoic; microbial mat; Liaoning region

check for updates

Citation: Zhang, Y.; Lai, G.; Gong, E.; Yuan, D.; Wilson, M.A.; Li, Y. Characteristics of Early Neoproterozoic Stromatolites from Southern Liaoning, North China: Insights into the Formation of Stromatolites. *J. Mar. Sci. Eng.* **2023**, *11*, 1709. https://doi.org/10.3390/jmse11091709

Academic Editor: George Kontakiotis

Received: 12 July 2023
Revised: 22 August 2023
Accepted: 28 August 2023
Published: 29 August 2023

1. Introduction

Stromatolites are sedimentary rocks characterized by lithified alternating laminae. Stromatolites are widely accepted as bio-sedimentary constructions formed by microbes such as cyanobacteria through binding and trapping sediments or inducing carbonate mineral precipitation [1–3]. The macrostructure of stromatolites includes columnar, domal, conical, hemispherical [4]. The microstructure of stromatolites is manifested in the laminae associated with microbial mats and non-microbial layers, the morphology of which is related to the type of layered microbial communities and characteristics of inorganic laminae [5,6]. Environmental factors are generally considered to control the morphology of the macrostructure, while microscopic features are typically attributed to microbial processes [5–14]. Stromatolites are widely found in Precambrian strata [2,15,16]. As the oldest fossils on Earth, stromatolites which grew influenced by the environment and microbial communities are keys to understanding the early evolution of life, paleogeography, paleoecology, and the atmosphere in the Precambrian. They also provide critical insights into the complex "carbonate factory" of the distant past [17,18].

Stromatolites in modern environments are relatively rare compared to the Precambrian and can be found in environmentally discrete settings [19]. There has been a long history of research on modern stromatolites, and examples reflect the diversity of modern stromatolites. (1) Large conical stromatolites that are composed of muddy sediments in Lake Untersee, Antarctica [20]. (2) Siliceous stromatolites from Yellowstone National Park in the USA and the Frying Pan Lake in North Island of New Zealand [21–23]. (3) Carbonate stromatolites from the Hamelin Pool in Shark Bay of Australia, the Little Darby Islands in the Bahamas, and the Lagoa Vermelha of southeastern Brazil [5,12,24–31]. Although differences occur among these modern stromatolites in morphology, size, components, and growth pattern, they can provide analogs for understanding the formation of ancient stromatolites as well as depositional environments, and they provide key insight into microbial biomineralization during stromatolite accretion [16,32,33].

The well-preserved Neoproterozoic stromatolites in southern Liaoning, China, are ideal fossil records for revealing the paleoenvironment, paleoecology, and microbial mineralization on the northeastern North China Craton [3,34]. Previous studies have investigated and analyzed the morphological classification of Ganjingzi stromatolites around Yuanjiagou village [7]. The construction processes as well as controlling factors of Ganjingzi stromatolite mounds/biostrome are discussed [7]. However, questions remain about the formation process of the Ganjingzi stromatolites. In this study we show more detailed descriptions of characteristics about the macro-/micro- morphology and present a comparison between Precambrian stromatolites from the Ganjingzi Formation and modern carbonate stromatolites, providing new perspectives on Precambrian stromatolite growth and laminae genesis.

2. Geological Setting

The study area is in southern Liaoning, in the northeast of the North China Craton (Figure 1). A continuous succession is well preserved in southern Liaoning including the Wuhangshan Group (Changlingzi, Nanguanling, and Ganjingzi formations) and the Jinxian Group (Yingchengzi, Shisanlitai, Majiatun, Cuijiatun, and Xingmincun formations), which were representative of shallow marine and tidal flat deposits composed of carbonates with siliciclastic debris [35]. The Wuhangshan and Jinxian groups in the southern Liaoning area are Tonian in age and range from 950 to 886 Ma according to the lithostratigraphic, biostratigraphic, chemostratigraphic, and radiometric geochronological data [36–38].

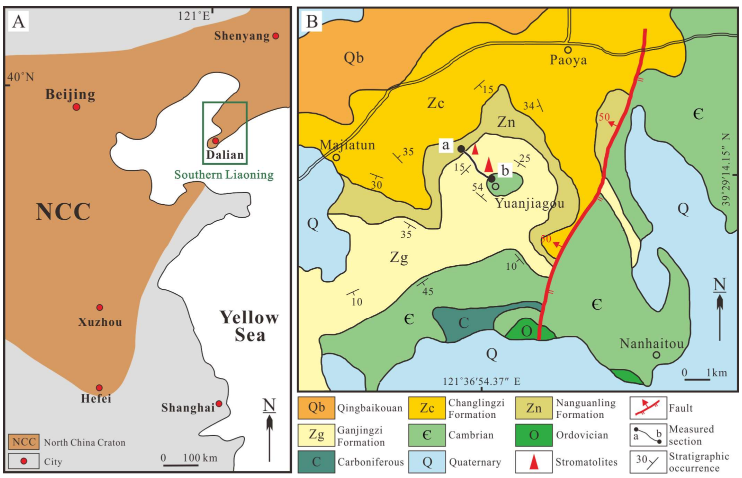

Figure 1. Geological setting of the study area. (**A**) The southern Liaoning located in the northeastern North China Craton. (**B**) Simplified geological map showing the location of the Ganjingzi Formation, measured section, and stromatolites.

The Ganjingzi Formation is well exposed around Yuanjiagou Village in Fuzhouwan Town, Dalian City, Liaoning Province, and is underlain by the Nanguanling Formation as well as overlain by the Cambrian Jianchang Formation, representing a set of tidal flat deposits [35]. The measured section is located in the northwest of Yuanjiagou Village; it is 266.1 m thick and is divided into three members (Figure 2). The Lower Member composed of light-to-dark lime-dolomite enriched in a fine-grained intraclastic sediment, and developed fenestrae representing an evaporative setting. The Middle Member is dominated by dark-gray to gray dolomitic limestone and dolostone. Horizontal- and wavy-bedded structures are developed. Some elements such as chert, siliciclast, carbonate debris, ooids, and tempestites are recorded in the field. The Upper Member is characterized by stromatolitic dolostone and the stromatolite columns that grow into biostrome.

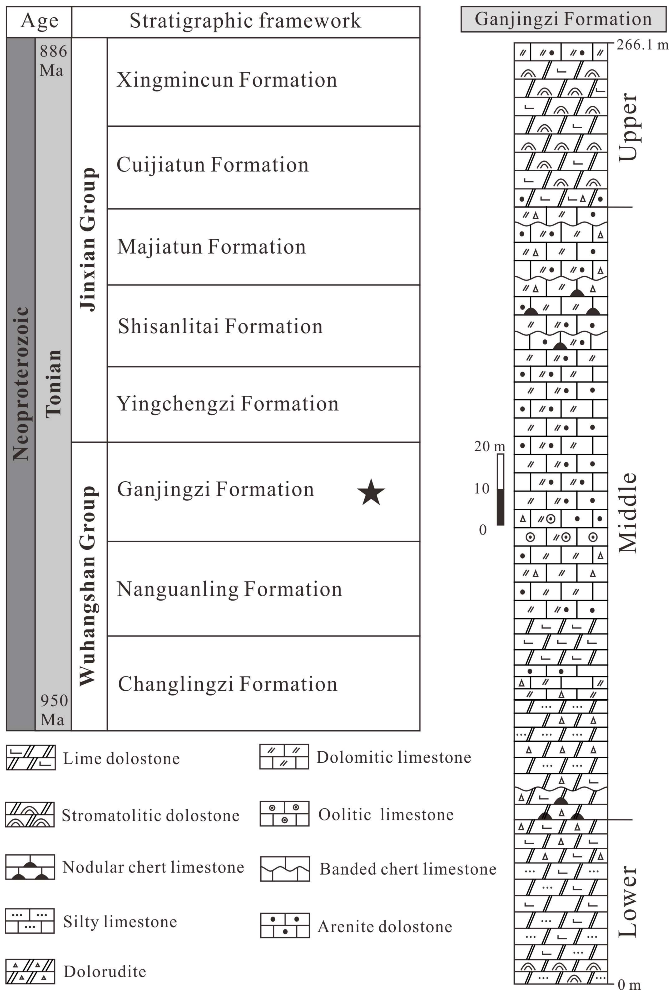

Figure 2. The stratigraphic framework of the early Neoproterozoic in southern Liaoning and a stratigraphic column of the Ganjingzi Formation (★) around Yuanjiagou Village (after Zhang et al. [7]). The asterisk indicates the studied formation in this work. Data for the age refer to Zhang et al. [37] and Zhang et al. [38].

Stromatolites in the Ganjingzi Formation are primarily preserved in the lower and upper members [7]. The lower stromatolite mounds are about 2 m thick and 1–3 m wide. The mounds can be divided into three growth stages. Stratiform stromatolites are the main form of stage I. Stage II is dominated by unbranched columnar stromatolites, while branched columns occur in stage III. The upper stromatolite biostrome extends laterally over several tens of meters and is about 27 m thick. Two growth stages of the biostrome in ascending order, the dispersed growth stage and dense clumping stage, are developed.

3. Materials and Methods

The Ganjingzi stromatolites were observed in the field. The lithology, morphology, synoptic relief, diameter, growth density, and substrate of the stromatolites were measured and documented in detail. Sixty-two samples for stromatolites and lithology were collected through the section of the Ganjingzi Formation. Twenty-four polished slabs (approximately 12 cm × 16 cm) were used for the analysis of stromatolite accretion and morphology. Moreover, 22 thin sections (approximately 5 cm × 2 cm) were prepared for lithology and stromatolite growth analysis. The polished slabs and thin sections were observed in detail under a microscope. The environment, morphological characteristics, and types of microbial mats were compared between the Ganjingzi stromatolites and the modern stromatolites. All samples of the Ganjingzi stromatolite are housed in the Department of Geology, Northeastern University, Shenyang, China.

4. Results

4.1. Macrostructure

The Ganjingzi stromatolites composed of dolostones are mainly developed in the Lower and Upper members and form stromatolite mounds and biostromes, respectively [7]. Most of the stromatolites are manifested as columnar, stratiform, and domal forms.

The initial stage of lower stromatolite mounds is typically comprised of stratiform microbial mats (Figure 3A). The Ganjingzi stratiform microbialites are composed of alternating bright laminae about 1 mm thick and dark laminae about 0.5–2 mm. Laminae are gentle and undulate with a relatively high degree of laminar inheritance. Laterally the laminae are discontinuous. The boundary between the dark and bright laminae is difficult to distinguish in some places. Pores and fenestrae structure are rare in the stratiform microbialites.

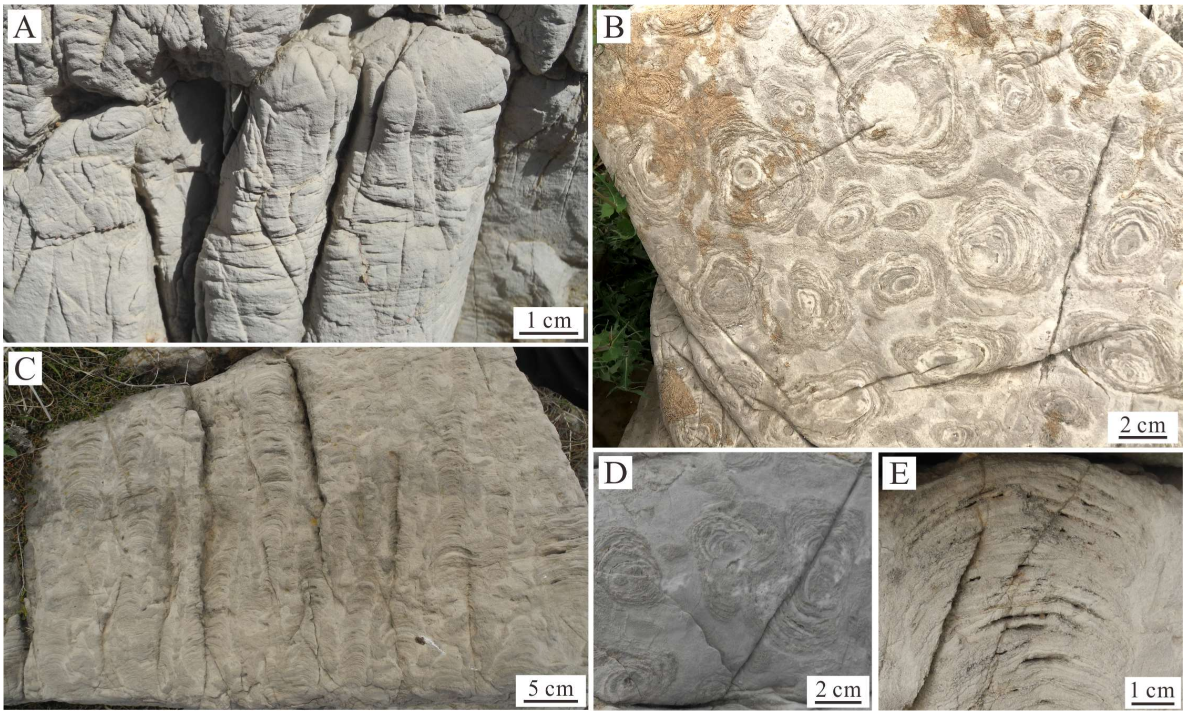

Figure 3. Characteristics of the Ganjingzi stromatolites observed in the field. (**A**) Stratiform microbialites. (**B**) Columnar stromatolites are manifested in elliptical-to-rounded shapes in the cross-section. (**C**) Columns from the dense clumping stage of the upper stromatolite biostrome are parallel, erect, and branched. (**D**) Columns are contiguous to closely spaced, forming aggregates of columns (right of the picture). (**E**) The pores and fenestrae structure are observed on the weathering surface of an unbranched columnar.

Columnar stromatolites are mainly preserved in the lower stromatolite mounds and the upper stromatolites biostrome in the study area. Columns occur as rough cylinders with generally elliptical-to-rounded shapes, or less frequently oblong in transverse outlines (Figure 3B). Most of the columns range from 2–10 cm in width and are less than 30 cm in relief (Figure 3C). The synoptic relief of a few double-branching columns can reach 65 cm. At the column margins, buds and protrusions can be observed on the wall. Spaces between columns are narrow and filled by variable-size and poorly sorted laminae fragments, frequently mixed with detrital sediments (Figure 4A–C). Due to the close spacing, columns are connected by bridges in some positions. The lateral overgrowth of columns may coalesce into large columns (Figure 3D). The pores and fenestrae structures developed between the laminae in part of the columns are more visible on the weathering surface and polished slabs (Figures 3E and 4D). The growth direction of columns is erect mostly, while some may change during accretion (Figure 4D). In order to better systematically present the diversity of columnar stromatolite morphologies, a total of seven sub-types are summarized and described (Table 1), which is the statistical result of the forms of numerous columns in the outcrop. The sizes of stromatolite columns of the same morphotype may differ.

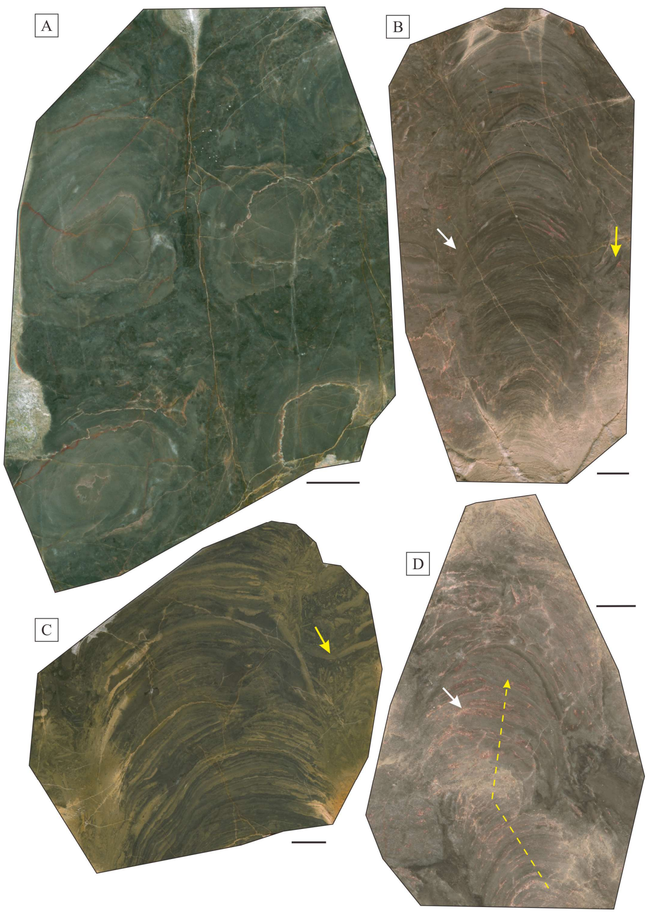

Figure 4. Polished slab of the stromatolite columns. The scale bar is 1 cm. (**A**) Cross-section of the columns. Around the columns the dark gray fragments of microbial mats mixed with poorly sorted debris. (**B**) Sub-type III columnar with good inheritance. The white arrow indicates the wall of the column and the yellow arrow shows the fragments of the microbial mats near the column. (**C**) Sub-type IV columnar. The yellow arrow indicates the poorly sorted fragments of the microbial mats. (**D**) Sub-type III columnar. The yellow dashed line represents the axis of stromatolite growth and the white arrow indicates the fenestrae structure filled by microspar between the laminae.

Table 1. Classification and description of the columnar stromatolites in the Ganjingzi Formation according to the differences of columnar width, relief, numbers of branching, branching angle, and position [7].

Types	Sub-Types	Columnar Description	Relief (cm)
Unbranched	I	Consistent width during accretion and narrows at the top	10–20
	II	Width increases to maximum and then decreases	<20
	III	Width gradually increases during accretion	20–30
	IV	Width remains the same in general	8–15
Branched	V	Parallel or minutely divergent branching	10–30
	VI	Markedly divergent branching	3–20
	VII	Double branching	<70

For the branched columnar forms, parallel or minutely divergent branching are the common types, while markedly divergent branching can be manifested in some small columns. Secondary columns can occur at any position of the primary columns and grow the random types described in Table 1. The unbranched stromatolites are mainly present in stages II and III of the lower stromatolite mounds, and the dispersed growth stage of the upper stromatolite biostrome. The branched columns are abundantly developed in stage III of the mounds and dense clumping stage of the biostrome.

Alternating light and dark laminae are the basis for the formation of the columns (Figure 4). In the polished slabs, laminae are symmetrical-to-asymmetrical with a relatively high degree of laminar inheritance and are manifested in an irregular relief. In some places, the laminae may inflect downward to form a wall over previous laminae at the column margins (Figure 4B). The thickness of the laminae is variable.

4.2. Microstructure

In the thin section, the Ganjingzi columnar stromatolites are composed of dark laminae (DL) dominated by dolomitic micrite and light laminae (LL) dominated by fine or medium dolomite (Figure 5A). Under a microscope, the laminae have an uneven thickness and relief. Dark laminae can be divided into two types by color, dark laminae I (DL-1) and dark laminae II (DL-2). Therefore, the tripartite lamina pattern of the columnar stromatolites can be illustrated (Figure 5B).

DL-1 in the columnar stromatolites from the lower stromatolite mounds may be well defined and relatively well preserved, and is composed of dense dark brown micrite, manifested in an irregular domal shape with an uneven thickness that mostly ranges from 1–2.5 mm. Sharp boundaries between laminae are observed. Some brown micrometer-sized spotted clots and peloids ranging from 40 to 160 μm are aggregated on the surface of DL-1 (Figure 5C). There is a link between the spotted clots and peloids and DL-1 according to the distribution and similarity in color. The remaining spaces and pores among the peloids are filled by microspar. The smaller thickness of the DL-1 with poorly continuous and variable forms can be recognized in columns from the upper stromatolite biostrome, with no evident rhythmicity (Figure 5D).

DL-2 consists of light brown fine dolomite; in the lower stromatolite mounds, DL-2 is morphologically similar to DL-1. The dark brown clots are frequently developed in the boundary between DL-2 and DL-1, and they can also be observed within DL-2. The poorly continuous DL-2 is the main type of dark laminae of columns in the upper stromatolite biostrome and the thickness of DL-2 ranges between 0.5 and 2 mm. There is a fuzzy boundary between different types of laminae (Figure 5B). DL-2 can reach the sides of the columns to form the wall (Figure 5E).

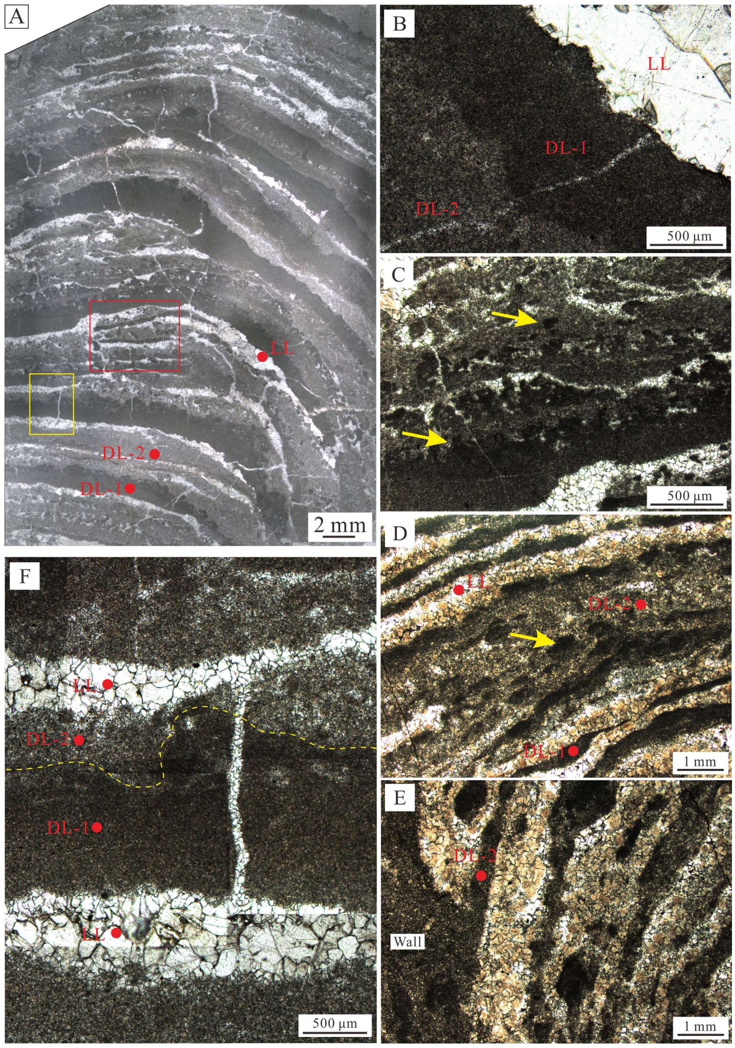

Figure 5. Microstructure of the Ganjingzi columnar stromatolites. (**A**) Tripartite lamina structure composed of dark laminae I (DL-1), dark laminae II (DL-2), and light laminae (LL). The morphologies of the laminae are inherited vertically. The yellow rectangle indicates (**F**). The red rectangle shows that some detrital microbreccia are developed within the dark laminae. (**B**) The three types of laminae are manifested in different colors. The sharp boundary can be shown among the laminae within the columns from the lower mounds. (**C**) The yellow arrow indicates the spotted clots and peloids on the surface of DL-1. (**D**) The laminae are discontinuous within the columns from the upper biostrome and the light laminae occupy a larger volume of the columns. The yellow arrow indicates the spotted clots. (**E**) The DL-2 is linked to the wall of columns from the upper biostrome, suggesting that the growth of DL-2 contributed to the formation of the wall. (**F**) Enlargement of the yellow rectangle in (**A**). Recrystallized grains within the light laminae and the fracture as a bridge between the LL.

The light laminae are composed of dolomite, representing the inorganic component of the Ganjingzi stromatolites. Laminar inheritance is good between LL and DL, and it is slightly convex. Polygonal recrystallized dolomite ranging from 0.2 to 1 mm can be observed in the laminae. In the lower stromatolite mounds, the light laminae are linked to the fractures that cut the dark laminae (Figure 5F). The fractures are filled by microspar and are 80 to 150 μm in width. However, a similar phenomenon is rarely manifested in the columns of the upper stromatolite biostrome, while the light laminae occupy a larger volume of the columns (Figure 5D).

4.3. Substrate

In the study area, the massive dolotone with marked topographic relief, indicating a hardground substrate, was suitable for stromatolites to colonize (Figure 6A,B). The columns accrete vertically from the substrate at the initial stage and gradually shift to upward growth subsequently (Figure 6C). The diameter of the columns increased during accretion. Spaces between the columns are filled with intraclasts.

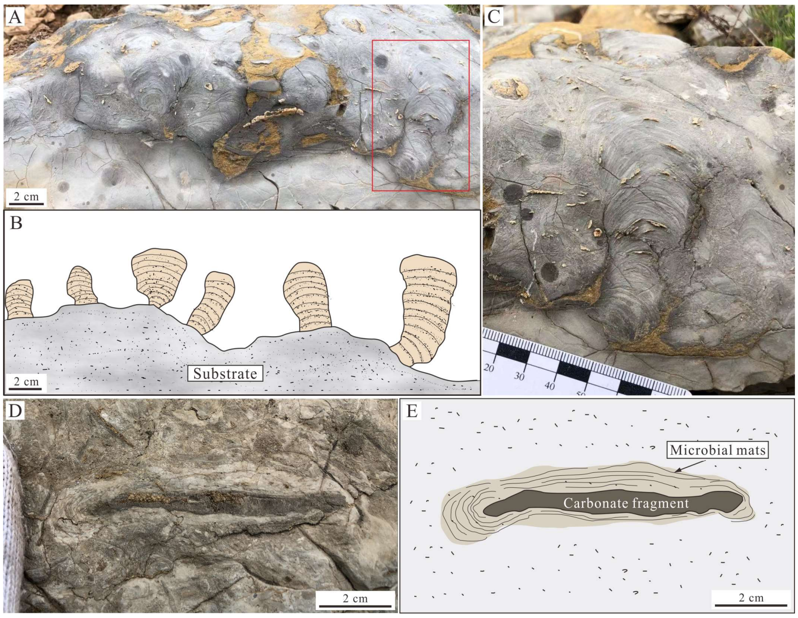

Figure 6. (**A**) Outcrop of the columnar stromatolites colonizing a high-relief hard substrate. The growth direction and width of the columns changed during the growth processes. (**B**) Reconstruction of (**A**). (**C**) Enlargement of the red rectangle in (**A**). (**D**) Microbes colonize on the oblong carbonate fragment and form stratiform sheet. (**E**) Reconstruction of (**D**).

Some centimeter-scale carbonate fragments with irregular shapes appear to be a suitable substrate for microbes to colonize (Figure 6D,E). The stratiform microbial mats grow around the fragment and form sheets with variable thickness variable of up to 1 cm. Distinct boundaries among the stratiform microbial mats, colonized fragment, and surrounding rock can be observed (Figure 6D). Laterally the laminae are discontinuous. The stromatolites formed by colonization on fragments have poorer laminar inheritance than those colonized on the hard substrate with topographic relief.

5. Discussion

5.1. Formation of the Ganjingzi Stromatolites

The formation of stromatolites is controlled partly by environmental factors and partly by the constituent microbial communities [5,39]. The lithology of the Ganjingzi stromatolites is dominated by dolostones, while the genesis of Precambrian dolomite is still uncertain, although various hypotheses have been proposed in recent years [40,41]. It is commonly accepted that the dolomite is deposited under evaporation [42–45]. The uniformly distributed fine-grained dolomite developed in the hardground substrate of the Ganjingzi stromatolites suggests that it may appear in a similar evaporation setting (Figure 7). The involvement of microbes is more favorable for dolomite precipitation [46].

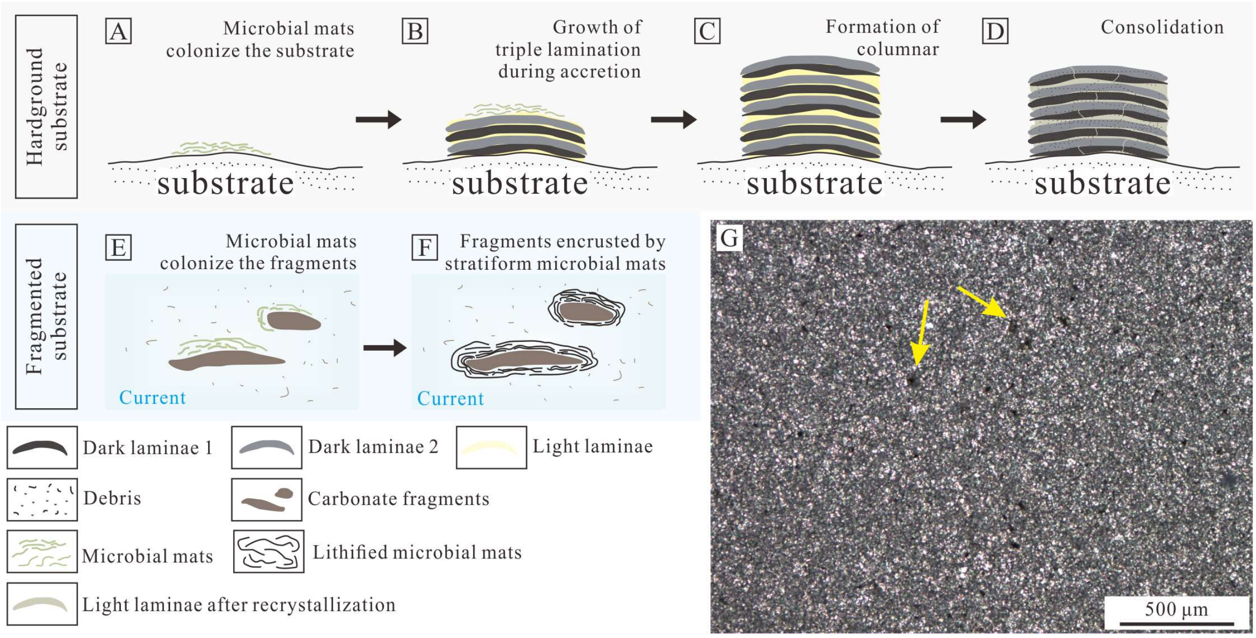

Figure 7. Formation pattern of the Ganjingzi stromatolites on hardground and fragmented substrate. (**A**) Microbes colonized the substrate and begin to build stromatolites. (**B**) Growth of columnar stromatolites with well-inherited tripartite lamina. The dark laminae associated with spotted clots were of microbial origin. The synsedimentary marine cement was involved to form light laminae during the forming process. (**C**) Stromatolites stopped growing and formed columns. (**D**) Recrystallization occurred during diagenesis and some fractures were developed. (**E**) Microbes colonized the carbonate fragments in the current. (**F**) The microbial mats grew around the fragments and encrustation. (**G**) Lithology of hardground substrate composed of uniformly distributed fine-grained dolomite. The yellow arrows indicate the spotted clots.

The growth pattern of the Ganjingzi stromatolites can be deciphered (Figure 7). In the Neoproterozoic, the southern Liaoning was in a restricted tidal-flat setting in the study area. The environment allowed microbes to colonize the flat or high-relief hardground substrate and build microbial mats (Figure 7A). The mats bound and trapped the sediments, or induced carbonate precipitation; these two types of mechanisms contributing to the upward growth of stromatolites [4,6] may be involved in the Ganjingzi stromatolites. The detrital particles were trapped or bound by microbial mats during accretion and preserved in the dark laminae (Figure 5A), while the dark laminae were composed of fine dolomite that precipitated in situ within the mats. In comparison to the former, the carbonate precipitating in situ contributed more to the formation of the laminae according to the volumes of the debris and fine-grained dolomite. DL-1 and DL-2 might correspond to two different types of microbial communities within the mats. Although the preservation of stromatolite-building microbes is difficult to identify from the geological history, the spotted clots and peloids textures were associated with a microbial origin [47]. The light laminae were the results of the spaces filled by synsedimentary marine cement between dark laminae because of their good inheritance. The stabilized topography gave rise to greater inheritance of shape for successive laminae [6]. The synsedimentary marine cement was able to support and stabilize the columns (Figure 7B). By the end of the accretion process, the columns were lithified (Figure 7C). During the diagenesis, minerals in the light laminae were recrystallized and formed coarser particles. Fractures were developed and cut through the dark laminae (Figure 7D).

The carbonate fragments provided a small hard substrate for microbes to colonize in the current. These poorly sorted fragments were potentially valuable resources for binding and boring organisms [48,49]. The variable thickness of the microbial mats surrounding the fragments indicated that the microbes were initially attached to parts of the fragments' surface (Figure 7E). After that, the fragments were enveloped by microbial mats and lithified (Figure 7F). The unstable fragments of the substrate moving in the current might have contributed to the poorly continuous inheritance of the laminae.

The diverse substrates contributed to the morphological diversity of the Ganjingzi stromatolites. The topography of the hard substrates that are stabilized and flat give rise to the erect shape of the stromatolite columns, and those that are rugged result in a shift in the direction of columnar growth (Figure 6C). The substrate's fragments mostly support the development of stratiform stromatolites. The current energy reflected by the hard fragments of the substrate is greater than that of the stabilized hardground substrate, suggesting that microbes adapt to various flows and substrates. The characteristics of the colonization substrate influenced the morphology of the stromatolites during their growth.

5.2. Comparison with Modern Stromatolites

Modern carbonate stromatolites provide analogs for revealing the formation processes of the Ganjingzi stromatolites and are well studied in the hypersaline Hamelin Pool and the Lagoa Vernelha lagoon (Figure 8). The morphology, mineral composition, and depositional environment of these modern carbonate stromatolites present opportunities for comparative sedimentological research advancing the understanding of the early Earth's surface conditions [12,24,50–52].

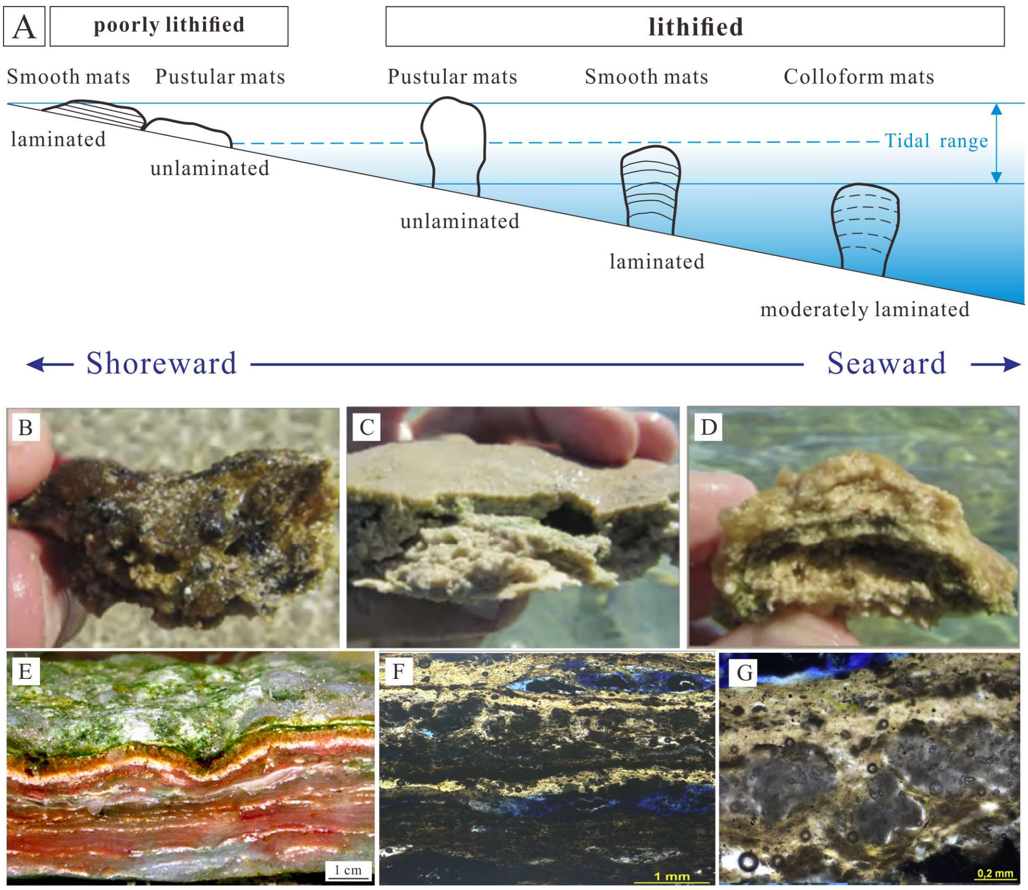

Figure 8. Characterization of the distribution, environment, and morphology of the modern carbonate stromatolites [5,8,24]. Note that photographs B to G are licensed. (**A**) Growth model of stromatolites in Hamelin Pool. (**B**) Pustular mat. (**C**) Smooth mat. (**D**) Colloform mat with domal structure. (**E**) Microbial mat from Lagoa Vermelha. The white stratified layers represent the carbonate precipitation; the green layer is dominated by cyanobacteria; the brown layers contain heterotrophic bacteria; the red layers contain purple sulphur bacteria. (**F**,**G**) The lithified stromatolites are mainly composed of carbonate peloids and micrite.

Hamelin Pool, Western Australia, represents a hypersaline setting because of the restricted seawater cycling, combined with high evaporation and low precipitation [29,30]. The Hamelin Pool stromatolites are distributed in the upper intertidal to subtidal region (Figure 8A). Common morphological types of stromatolites are stratiform, columnar, dome, and ridged. Poorly lithified stratiform stromatolites mainly grow in the upper intertidal, while the lower intertidal and subtidal stromatolites are composed of lithified microbial mats, manifested in various morphologies (Figure 8A) [5]. The irregular fenestrae structure can be seen between the laminae of uneven thickness in some lithified columnar stromatolite and are partly filled by marine cement [30]. Three reported types of microbial mats are mostly pustular, smooth, and colloform mats (Figure 8B–D) [5,53,54]. Notably, the laminae of the pustular mat as well as the smooth mat are manifested in various colors due to the difference in the microbial communities [8]. Two types of microbial micrite are observed within Hamelin Pool's stromatolites, red-brown micrite and gray peloidal micrite [5]. The microbial micrite forms laminae and clots in stromatolites, in some cases cementing accreted sediment grains.

Lagoa Vermelha is located in southeastern Brazil and is characterized by high evaporative and hypersaline conditions [24,50]. Studies of the Lagoa Vermelha stromatolites covering the morphology, microbial communities, growth environment, metabolism, biomineralization, and laminae genesis have been published over the last two decades [12,24,50,55,56]. The Lagoa Vermelha microbial mats are composed of white layers of carbonate precipitation alternating with non-lithified organic layers that contain various microbial communities, including autotrophic as well as heterotrophic bacteria [12]. The green, brown, and red layers of the microbial mats represent different microbial communities (Figure 8E) [24]. A peloidal microfabric texture preserved between the laminae in the lithified stromatolite was observed (Figure 8F,G). The remaining spaces are filled with microspar [24,51]. Various processes take place in the microbial mat, such as cyanobacteria photosynthesis and heterotrophic sulfate reduction [50,57].

The Ganjingzi stromatolites are comparable to modern carbonate stromatolites in macro-/micro- morphology and depositional settings (Table 2). The Ganjingzi stromatolites are manifested in various shapes such as stratiform, domal, and columnar, which also can be observed in the Hamelin Pool; Lagoa Vermelha is dominated by stratiform stromatolites. Furthermore, the uneven thickness of laminae and the irregular fenestrae structures are developed in both the Hamelin Pool stromatolites and the Ganjingzi stromatolites (Figure 3E) [30]. Peloidal microfabrics are also developed between laminae among the stromatolites from three regions, although there are differences in the preserved forms. The Ganjingzi stromatolites are composed of dolostone that may form in the tidal-lagoon system with high evaporation, comparable to the setting of Hamelin Pool and Lagoa Vermelha. The comparative study suggests that the stromatolites of Hamelin Pool and Lagoa Vermelha are a suitable analog of the Ganjingzi stromatolites. The formation of stromatolites from Hamelin Pool and Lagoa Vermelha is the result of microbial metabolism, photosynthesis, and biomineralization, which may be applied in the Ganjingzi stromatolites. Two types of dark laminae of Ganjingzi stromatolites may represent different microbial communities. Microbial photosynthesis and metabolism are hypothesized to play a key role during stromatolite accretion, but a more detailed discussion needs further research.

Table 2. Comparison of the Ganjingzi stromatolites from southern Liaoning, to the modern carbonate stromatolites from Hamelin pool and Lagoa Vermelha. The information of Hamelin pool and Lagoa Vermelha are from Suosaari et al., Playford and Cockbain, Allen et al., Reid et al., Vasconcelos et al., Delfino et al., and Spadafora et al. [5,8,12,24,29,30].

Stromatolite	Environment	Morphology	Microfabrics	Laminae Constituted
Ganjingzi (this study)	Tidal-flat setting with evaporation	Stratiform, dome, and columnar with fenestrae structure	Spotted clots and peloids aggregate	The tripartite lamina structure composed of two types of dark laminae and the light laminae
Hamelin Pool	Tidal-flat with hypersaline, high evaporation, low precipitation, and restricted seawater cycling	Stratiform, dome, ridged, and columnar with fenestrae structure	Two types of microbial micrite, red-brown micrite and gray peloidal micrite	Three types of microbial mats are pustular, smooth, colloform mats respectively.
Lagoa Vermelha	High evaporative and hypersaline conditions in the restricted lagoon	Stratiform and dome	Peloids and micritic lumps	The green, brown, and red layers of the microbial mats, together with the white layers of carbonate precipitation

6. Conclusions

The following conclusions are drawn based on the detailed observation of the outcrops, polished slab, and thin sections of the Ganjingzi stromatolites, and in reference to the genesis of modern carbonate stromatolites from Hamelin Pool (Shark Bay, Western Australia) and Lagoa Vermelha (Brazil).

(1) A tripartite lamina structure consisting of light laminae and two types of dark laminae is developed in the Ganjingzi stromatolites. Preservation of the spotted clots and peloids indicates that the genesis of dark laminae is linked to microbes, while the light laminae is the result of synsedimentary marine cement filling. Recrystallization occurred during diagenesis, leading to the enlargement of particles within the light laminae.

(2) The microbial mats in the study area colonize the topographic relief of both hardground and carbonate fragments, which influence the morphological diversity of the Ganjingzi stromatolites. The hardground substrate is suitable for the growth of columnar and stratiform stromatolites, while the hard fragments are mainly colonized by stratiform forms. The substrate is a key factor affecting the growth of stromatolites in the northeastern margin of the North China Craton during the Neoproterozoic.

(3) The environment, morphology, microfabrics, and laminae of the Ganjingzi stromatolite are comparable to those in the Hamelin Pool and Lagoa Vermelha, probably showing that the modern carbonate stromatolites are analogs for the Ganjingzi stromatolites. A similar genesis mechanism, biomineralization, and microbial metabolism of the modern stromatolites may be present in the stromatolites from the study area.

Author Contributions: Conceptualization, Y.Z., G.L. and E.G.; methodology, Y.Z. and G.L.; software, G.L. and Y.L.; validation, Y.Z., G.L., E.G. and M.A.W.; investigation, Y.Z., G.L. and D.Y.; resources, Y.Z. and E.G.; data curation, G.L.; writing—original draft preparation, Y.Z. and G.L.; writing—review and editing, Y.Z., G.L., E.G., D.Y., M.A.W. and Y.L.; visualization, Y.Z., G.L. and D.Y.; supervision, Y.Z. and E.G.; project administration, Y.Z., G.L. and E.G.; funding acquisition, Y.Z. and E.G. All authors have read and agreed to the published version of the manuscript.

Funding: This research was funded by the National Natural Science Foundation of China, grant numbers 42272008 and 41972002.

Institutional Review Board Statement: Not applicable.

Informed Consent Statement: Not applicable.

Data Availability Statement: Not applicable.

Acknowledgments: We sincerely thank the editors and reviewers for their insightful and constructive comments that significantly improved the manuscript.

Conflicts of Interest: The authors declare that they have no conflict of interest.

References

1. Riding, R. Microbial carbonates: The geological record of calcified bacterial-algal mats and biofilms. *Sedimentology* **2000**, *47*, 179–214. [CrossRef]
2. Awramik, S.M.; Sprinkle, J. Proterozoic stromatolites: The first marine evolutionary biota. *Hist. Biol.* **1999**, *13*, 241–253. [CrossRef]
3. Cao, R.J.; Yuan, X.L. *Stromatolites*; University of Science and Technology of China Press: Hefei, China, 2006; pp. 1–383.
4. Bosak, T.; Knoll, A.H.; Petroff, A.P. The meaning of stromatolites. *Annu. Rev. Earth Planet. Sci.* **2013**, *41*, 21–44. [CrossRef]
5. Suosaari, E.P.; Reid, R.P.; Playford, P.E.; Foster, J.S.; Stolz, J.F.; Casaburi, G.; Hagan, P.D.; Chirayath, V.; Macintyre, I.G.; Planavsky, N.J.; et al. New multi-scale perspectives on the stromatolites of Shark Bay, Western Australia. *Sci. Rep.* **2016**, *6*, 20557. [CrossRef] [PubMed]
6. Grotzinger, J.P.; Knoll, A.H. STROMATOLITES in PRECAMBRIAN CARBONATES: Evolutionary Mileposts or Environmental Dipsticks? *Annu. Rev. Earth Planet. Sci.* **1999**, *27*, 313–358. [CrossRef]
7. Zhang, Y.L.; Lai, G.M.; Gong, E.P.; Wilson, M.A.; Huang, W.T.; Guan, C.Q.; Yuan, D.C. Early Neoproterozoic well-preserved stromatolites from southern Liaoning, North China: Characteristics and paleogeographic implications. *Palaeoworld* **2023**, *32*, 1–13. [CrossRef]
8. Allen, M.A.; Goh, F.; Burns, B.P.; Neilan, B.A. Bacterial, archaeal and eukaryotic diversity of smooth and pustular microbial mat communities in the hypersaline lagoon of Shark Bay. *Geobiology* **2009**, *7*, 82–96. [CrossRef]
9. Jahnert, R.J.; Collins, L.B. Significance of subtidal microbial deposits in Shark Bay, Australia. *Mar. Geol.* **2011**, *286*, 106–111. [CrossRef]
10. Planavsky, N.; Grey, K. Stromatolite branching in the Neoproterozoic of the Centralian Superbasin, Australia: An investigation into sedimentary and microbial control of stromatolite morphology. *Geobiology* **2008**, *6*, 33–45. [CrossRef]
11. Suosaari, E.P.; Reid, R.P.; Oehlert, A.M.; Playford, P.E.; Steffensen, C.K.; Andres, M.S.; Suosaari, G.V.; Milano, G.R.; Eberli, G.P. Stromatolite provinces of hamelin pool: Physiographic controls on stromatolites and associated lithofacies. *J. Sediment. Res.* **2019**, *89*, 207–226. [CrossRef]
12. Vasconcelos, C.; Warthmann, R.; Mckenzie, J.A.; Visscher, P.T.; Bittermann, A.G.; Lith, Y. Lithifying microbial mats in Lagoa Vermelha, Brazil: Modern Precambrian relics? *Sediment. Geol.* **2006**, *185*, 175–183. [CrossRef]
13. Lepot, K.; Benzerara, K.; Brown, G.E.; Philippot, P. Microbially influenced formation of 2,724-million-year-old stromatolites. *Nat. Geosci.* **2008**, *1*, 118–121. [CrossRef]
14. Hickman-Lewis, K.; Cavalazzi, B.; Giannoukos, K.; D'Amico, L.; Vrbaski, S.; Saccomano, G.; Dreossi, D.; Tromba, G.; Foucher, F.; Brownscombe, W.; et al. Advanced two-and three-dimensional insights into Earth's oldest stromatolites (ca. 3.5 Ga): Prospects for the search for life on Mars. *Geology* **2022**, *51*, 33–38. [CrossRef]
15. Riding, R. The Nature of Stromatolites: 3500 Million Years of History and a Century of Research. In *Advances in Stromatolite Geobiology*; Reitner, J., Quéric, N., Arp, G., Eds.; Springer: Berlin/Heidelberg, Germany, 2011; pp. 29–74. [CrossRef]
16. Riding, R. Microbial carbonate abundance compared with fluctuations in metazoan diversity over geological time. *Sediment. Geol.* **2006**, *185*, 229–238. [CrossRef]
17. Wu, Y.S.; Jiang, H.X.; Li, Y.; Yu, G.L. Microfabric features of microbial carbonates: Experimental and natural evidence of mold holes and crusts. *J. Palaegeogr.* **2021**, *10*, 19. [CrossRef]
18. Kuang, H.W.; Fan, Z.X.; Liu, Y.Q.; Peng, N.; Zhu, Z.C.; Yang, Z.R.; Wang, Z.X.; Yu, H.L.; Zhong, Q. Stromatolite characteristics of Mesoproterozoic Shennongjia Group in the northern margin of Yangtze Block, China. *China Geol.* **2019**, *2*, 364–381. [CrossRef]
19. Reid, R.P.; Foster, J.S.; Radtke, G.; Golubic, S. Modern marine stromatolites of little darby island, exuma archipelago, bahamas: Environmental setting, accretion mechanisms and role of euendoliths. In *Advances in Stromatolite Geobiology*; Reitner, J., Quéric, N., Arp, G., Eds.; Springer: Berlin/Heidelberg, Germany, 2011; pp. 77–89. [CrossRef]
20. Andersen, D.T.; Sumner, D.Y.; Hawes, I.; Webster-Brown, J.; Mckay, C.P. Discovery of large conical stromatolites in Lake Untersee, Antarctica. *Geobiology* **2011**, *9*, 280–293. [CrossRef] [PubMed]
21. Bosak, T.; Bush, J.W.M.; Flynn, M.R.; Liang, B.; Ono, S.; Petroff, A.P.; Sim, M.S. Formation and stability of oxygen-rich bubbles that shape photosynthetic mats. *Geobiology* **2010**, *8*, 45–55. [CrossRef]
22. Bosak, T.; Liang, B.; Sim, M.S.; Petroff, A.P. Morphological record of oxygenic photosynthesis in conical stromatolites. *Proc. Natl. Acad. Sci. USA* **2009**, *106*, 10939–10943. [CrossRef]
23. Petroff, A.P.; Sim, M.S.; Maslov, A.; Krupenin, M.; Rothman, D.H.; Bosak, T. Biophysical basis for the geometry of conical stromatolites. *Proc. Natl. Acad. Sci. USA* **2010**, *107*, 9956–9961. [CrossRef]

24. Delfino, D.O.; Wanderley, M.D.; Silva e Silva, L.H.; Feder, F.; Lopes, F.A.S. Sedimentology and temporal distribution of microbial mats from Brejo do Espinho, Rio de Janeiro, Brazil. *Sediment. Geol.* **2012**, *263–264*, 85–95. [CrossRef]
25. Awramik, S.M.; Riding, R. Role of algal eukaryotes in subtidal columnar stromatolite formation. *Proc. Natl. Acad. Sci. USA* **1988**, *85*, 1327–1329. [CrossRef] [PubMed]
26. Burns, B.P.; Anitori, R.; Butterworth, P.; Henneberger, R.; Goh, F.; Allen, M.A.; Ibañez-Peral, R.; Bergquist, P.L.; Walter, M.R.; Neilan, B.A. Modern analogues and the early history of microbial life. *Precambrian Res.* **2009**, *173*, 10–18. [CrossRef]
27. Dravis, J.J. Hardened subtidal stromatolites, Bahamas. *Science* **1983**, *219*, 385–386. [CrossRef] [PubMed]
28. Logan, B.W. Cryptozoon and associate stromatolites from the Recent, Shark Bay, Western Australia. *J. Geol.* **1961**, *69*, 517–533. [CrossRef]
29. Reid, R.P.; James, N.P.; Macintyre, I.G.; Dupraz, C.P.; Burne, R.V. Shark Bay stromatolites: Microfabrics and reinterpretation of origins. *Facies* **2003**, *49*, 299–324. [CrossRef]
30. Playford, P.E.; Cockbain, A.E. Modern Algal Stromatolites at Hamelin Pool, a Hypersaline Barred Basin in Shark Bay, Western Australia. In *Developments in Sedimentology*; Walter, M.R., Ed.; Elsevier Scientific Publishing Company: Amsterdam, The Netherlands, 1976; Volume 20, pp. 389–411. [CrossRef]
31. Reid, R.P.; Visscher, P.T.; Decho, A.W.; Stolz, J.F.; Bebout, B.M.; Dupraz, C.; Macintyre, I.G.; Paerl, H.W.; Pinckney, J.L.; Prufert-Bebout, L.; et al. The role of microbes in accretion, lamination and early lithification of modern marine stromatolites. *Nature* **2000**, *406*, 989–992. [CrossRef]
32. Riding, R. Structure and composition of organic reefs and carbonate mud mounds: Concepts and categories. *Earth-Sci. Rev.* **2002**, *58*, 163–231. [CrossRef]
33. Mei, M.X.; Meng, Q.F. Composition diversity of modern stromatolites: A key and window for further understanding of the formation of ancient stromatolites. *J. Palaegeogr.* **2016**, *18*, 127–146. (In Chinese)
34. Hua, H.; Cao, R.J. Neoproterozoic stromatolite assemblages from the Shisanlitai Stage and its significance in the regional and continental correlation. *J. Stratigr.* **2003**, *27*, 19–25. (In Chinese)
35. Bureau of Geology and Mineral Resources of Liaoning Province. *Regional Geology of Liaoning Province*; Geological Publishing House: Beijing, China, 1989; p. 856. (In Chinese)
36. Pang, K.; Tang, Q.; Wan, B.; Li, G.J.; Chen, L.; Yuan, X.L.; Zhou, C.M. Integrated Meso-Neoproterozoic stratigraphy in the Jiao-LiaoXu-Huai area of North China Craton: A review. *J. Stratigr.* **2021**, *45*, 467–492. (In Chinese)
37. Zhang, S.; Zhao, Y.; Ye, H.; Hu, G. Early Neoproterozoic emplacement of the diabase sill swarms in the Liaodong Peninsula and pre-magmatic uplift of the southeastern North China Craton. *Precambrian Res.* **2016**, *272*, 203–225. [CrossRef]
38. Zhang, Z.; Peng, P.; Feng, L.; Gong, Z.; Mitchell, R.N.; Li, Y. Oldest-known Neoproterozoic carbon isotope excursion: Earlier onset of Neoproterozoic carbon cycle volatility. *Gondwana Res.* **2021**, *94*, 1–11. [CrossRef]
39. Rishworth, G.M.; van Elden, S.; Perissinotto, R.; Miranda, N.A.F.; Steyn, P.; Bornman, T.G. Environmental influences on living marine stromatolites: Insights from benthic microalgal communities. *Environ. Microbiol.* **2016**, *18*, 503–513. [CrossRef] [PubMed]
40. Chang, B.; Li, C.; Liu, D.; Foster, I.; Tripati, A.; Lloyd, M.K.; Maradiaga, I.; Luo, G.M.; An, Z.H.; She, Z.B.; et al. Massive formation of early diagenetic dolomite in the Ediacaran ocean: Constraints on the "dolomite problem". *Proc. Natl. Acad. Sci. USA* **2020**, *117*, 14005. [CrossRef] [PubMed]
41. Kuang, H.W.; Liu, Y.Q.; Peng, N.; Vandyk, T.M.; Le Heron, D.P.; Zhu, Z.C.; Bai, H.Q.; Wang, Y.C.; Wang, Z.X.; Zhong, Q.; et al. Ediacaran cap dolomite of Shennongjia, northern Yangtze Craton, South China. *Precambrian Res.* **2022**, *368*, 106483. [CrossRef]
42. Gregg, J.M.; Bish, D.L.; Kaczmarek, S.E.; Machel, H.G. Mineralogy, nucleation and growth of dolomite in the laboratory and sedimentary environment: A review. *Sedimentology* **2015**, *62*, 1749–1769. [CrossRef]
43. Compton, J.; Harris, C.; Thompson, S. Pleistocene dolomite from the namibian shelf: High $^{87}Sr/^{86}Sr$ and $\delta^{18}O$ values indicate an evaporative, Mixed-Water origin. *J. Sediment. Res.* **2001**, *71*, 800–808. [CrossRef]
44. Hofbauer, B.; Viehmann, S.; Gier, S.; Bernasconi, S.M.; Meister, P. Microfacies and C/O-isotopes in lacustrine dolomites reflect variable environmental conditions in the Germanic Basin (Arnstadt Formation, Upper Triassic). *Austrian J. Earth Sci.* **2021**, *114*, 66–87. [CrossRef]
45. Wu, Y.; Wu, Z. Diagenetic modification of dolomite in middle Ordovician carbonates, Taiyuan City area, China. *Sediment. Geol.* **1998**, *116*, 143–156. [CrossRef]
46. Roberts, J.A.; Bennett, P.C.; González, L.A.; Macpherson, G.L.; Milliken, K.L. Microbial precipitation of dolomite in methanogenic groundwater. *Geology* **2004**, *32*, 277–280. [CrossRef]
47. Flügel, E. Microfacies data: Matrix and grains. In *Microfacies of Carbonate Rocks: Analysis, Interpretation and Application*, 2nd ed.; Flügel, E., Ed.; Springer: Berlin/Heidelberg, Germany, 2010; pp. 73–176. [CrossRef]
48. Wilson, M.A. Ecological dynamics on pebbles, cobbles, and boulders. *Palaios* **1987**, *2*, 594–599. [CrossRef]
49. Zhang, Y.; Gong, E.; Wilson, M.A.; Guan, C.; Sun, B.; Chang, H. Paleoecology of a Pennsylvanian encrusting colonial rugose coral in south Guizhou, China. *Paleogeogr. Paleoclimatol. Paleoecol.* **2009**, *280*, 507–516. [CrossRef]
50. Keim, C.N.; Dos Santos, H.N.; Santiago, C.S.; Pennafirme, S.; Neumann, R.; Schnellrath, J.; Lima, I.; Crapez, M.A.C.; Farina, M. Microstructure and mineral composition of Holocene stromatolites from Lagoa Vermelha, a hypersaline lagoon in Brazil: Insights into laminae genesis. *J. Sediment. Res.* **2020**, *90*, 887–905. [CrossRef]
51. Spadafora, A.; Perri, E.; Mckenzie, J.A.; Vasconcelos, C. Microbial biomineralization processes forming modern Ca:Mg carbonate stromatolites. *Sedimentology* **2010**, *57*, 27–40. [CrossRef]

52. Dupraz, C.; Reid, R.P.; Braissant, O.; Decho, A.W.; Norman, R.S.; Visscher, P.T. Processes of carbonate precipitation in modern microbial mats. *Earth-Sci. Rev.* **2009**, *96*, 141–162. [CrossRef]
53. Hoffman, P. Stromatolite Morphogenesis in Shark Bay, Western Australia. In *Developments in Sedimentology*; Walter, M.R., Ed.; Elsevier Scientific Publishing Company: Amsterdam, The Netherlands, 1976; Volume 20, pp. 261–271. [CrossRef]
54. Edgcomb, V.P.; Bernhard, J.M.; Summons, R.E.; Orsi, W.; Beaudoin, D.; Visscher, P.T. Active eukaryotes in microbialites from Highborne Cay, Bahamas, and Hamelin Pool (Shark Bay), Australia. *ISME J.* **2014**, *8*, 418–429. [CrossRef]
55. Carvalho, C.; Oliveira, M.I.N.; Macario, K.; Guimarães, R.B.; Keim, C.N.; Sabadini-Santos, E.; Crapez, M.A.C. Stromatolite growth in Lagoa Vermelha, southeastern coast of Brazil: Evidence of environmental changes. *Radiocarbon* **2018**, *60*, 383–393. [CrossRef]
56. Areias, C.; Barbosa, C.F.; Cruz, A.P.S.; Mckenzie, J.A.; Ariztegui, D.; Eglinton, T.; Haghipour, N.; Vasconcelos, C.; Sánchez-Román, M. Organic matter diagenesis and precipitation of Mg-rich carbonate and dolomite in modern hypersaline lagoons linked to climate changes. *Geochim. Cosmochim. Acta* **2022**, *337*, 14–32. [CrossRef]
57. Warthmann, R.; Vasconcelos, C.; Bittermann, A.G.; Mckenzie, J.A. The role of purple sulphur bacteria in carbonate precipitation of modern and possibly early Precambrian stromatolites. In *Advances in Stromatolite Geobiology*; Reitner, J., Quéric, N., Arp, G., Eds.; Springer: Berlin/Heidelberg, Germany, 2011; pp. 141–149. [CrossRef]